Chemiluminescence of 1,1′-biisoquinolinium and 2,2′-biquinolinium salts. Reactions of electron-rich olefins with molecular oxygen

Yukie Mori,* Kumiko Isozaki and Koko Maeda

Department of Chemistry, Faculty of Science, Ochanomizu University, Otsuka, Bunkyo-ku, Tokyo 112, Japan

2,2′-Dialkyl-1,1′-biisoquinolylidenes (BIQ), having been prepared by two-electron reduction of the corresponding diquaternary salts $BIQ^{2+}(X^-)_2$, react with triplet dioxygen to produce chemiluminescence (CL). In aprotic solvents, the kinetics of the reaction are first-order with respect to the concentrations of the substrate and of oxygen. The second-order rate constants at 25 °C increase in the order DMF < MeCN < DMSO, which correlate with the free energy change for an electron-transfer (ET) from BIQ to O_2, although this process is endothermic in all three solvents. In non-polar solvents such as benzene, the reaction proceeds much more slowly. From these results, a reaction mechanism is proposed as follows. An ET or partial charge-transfer gives a radical ion pair $\{BIQ^{\cdot+} \cdots O_2^{\cdot-}\}$ or a CT complex, in which intersystem crossing takes place from the triplet to the singlet state, and then radical coupling at the 1-position followed by cyclisation yields a 1,2-dioxetane, the postulated intermediate of the CL reaction. An electron-rich olefin having a closely related structure, 1,1′-dimethyl-2,2′-bisquinolylidene (BQ), shows a similar redox behaviour to that of BIQ. Reaction of BQ with O_2 produces CL, and the emitter has been identified as the singlet excited state of 1-methyl-2(1*H*)-quinolinone 8a. The effects of substituents in the quinoline ring on the autoxidation rate have been investigated in MeCN and DMSO. An olefin having the more negative oxidation potential shows the higher reactivity to O_2, suggesting that the autoxidation of BQ should take place *via* a similar reaction pathway as that of BIQ.

It was reported that 2,2′-ethylene-1,1′-biisoquinolinium dibromide $\mathbf{1}^{2+}(Br^-)_2$ produced a chemiluminescence (CL) on addition of base and hydrogen peroxide in hydroxylic solvents.[1–3] Recently, we reinvestigated the CL reaction of $\mathbf{1}^{2+}$ in aprotic solvents and proposed that the two-electron reduced species **1** reacted with molecular oxygen to give a 1,2-dioxetane intermediate, thermal decomposition of which generated the excited singlet state of 2,2′-ethylene-bis[1(2*H*)-isoquinolinone] **4** as the emitter (Scheme 1).[4] Trimethylene-bridged analogue $\mathbf{2}^{2+}(Br^-)_2$ and an unbridged system $\mathbf{3}^{2+}(I^-)_2$ also exhibited CL under similar conditions, although the intensity was lower than that for $\mathbf{1}^{2+}$. The crucial factors controlling reactivity to O_2 and CL quantum yield for this system have not yet been clarified. The dihedral angles between the two isoquinoline planes are different among $\mathbf{1}^{2+}$–$\mathbf{3}^{2+}$,[5,6] which probably affects the electronic structure and the reactivity of the reduced species.

Addition of triplet dioxygen to a C=C double bond in the singlet state olefin is spin-forbidden. In the reaction of an electron-rich olefin with O_2, a spin inversion process can take place *via* a charge-transfer (CT) complex.[7] Alternatively, an active oxygen species, such as $O_2^{\cdot-}$, ·OOH or $^1O_2$, may be formed as an intermediate. Thummel *et al*. reported cycloaddition of molecular oxygen to a C=C bond in diimidazolinylidenes, but no reaction mechanism was described.[8] In order to clarify a detailed mechanism of the reaction of such electron-rich olefins with O_2, a more systematic, quantitative investigation is required. In the present study, we have investigated the kinetics of oxygenation of electron-rich olefin **1** in various solvents and proposed involvement of an electron transfer (ET) or a charge transfer (CT) process in the rate determining step. As a closely related system, the redox properties and CL reaction of 2,2′-biquinolinium (BQ^{2+}) salts have been examined. The structures and spin density distribution of radical cations $BIQ^{\cdot+}$ and $BQ^{\cdot+}$, plausible intermediates of the CL reaction, are also discussed on the basis of EPR and NMR spectra and semi-empirical MO calculations.

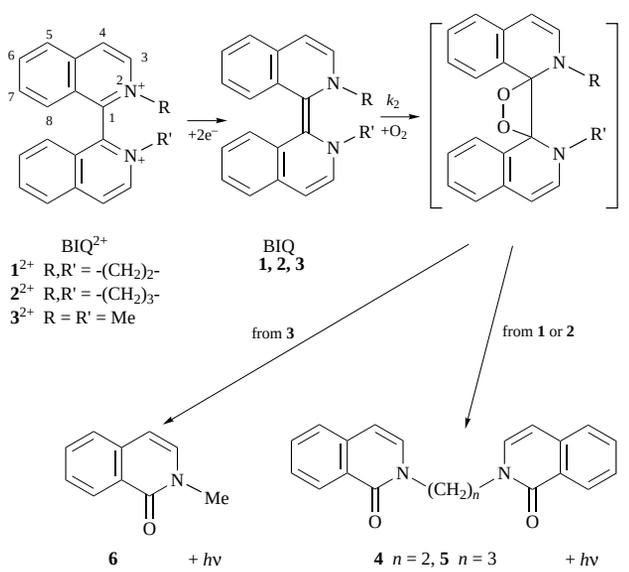

Scheme 1

Results and discussion

CL efficiency of BIQ^{2+} salts

In the CL reaction of BIQ^{2+} salts with alkaline hydrogen peroxide in MeOH–H_2O, $\mathbf{1}^{2+}$ produced the most intense light among the three. The ratio of the integrated CL intensity was $\mathbf{1}^{2+}:\mathbf{2}^{2+}:\mathbf{3}^{2+} = 1:0.1:0.02$. The order of $\mathbf{1}^{2+} > \mathbf{2}^{2+} > \mathbf{3}^{2+}$ was in agreement with the results reported by Mason and Roberts.[1] The difference in the CL efficiency, however, does not necessarily reflect the difference in the yield of the singlet excited state. The chemical yield of **4** from $\mathbf{1}^{2+}(Br^-)_2$ was *ca*. 90%, while

* *Present address:* Molecular Photochemistry Laboratory, The Institute of Physical and Chemical Research (RIKEN), Wako, Saitama, 351-01, Japan.
E-Mail ymori@postman.riken.go.jp

Table 1 Redox potentials $E^{\circ\prime}$ (V *vs.* Ag/Ag^+) in various solvents[a]

Compd.	MeCN	DMF	DMSO
$\mathbf{1}^{2+}$	−0.42, −0.80	−0.51, −0.81	−0.57, −0.86
$\mathbf{2}^{2+}$	−0.645, −0.945	−0.73, −0.96	−0.79, −1.00
$\mathbf{3}^{2+}$	−0.82, −0.93	−0.93	−0.98
$\mathbf{7a}^{2+}$	−0.57, −0.72	−0.66, −0.72	−0.735
$\mathbf{7b}^{2+}$	−0.62, −0.78	−0.705, −0.78	−0.785
$\mathbf{7c}^{2+}$	−0.68, −0.79	−0.77	−0.81
O_2	−1.20	−1.25	−1.16

[a] 0.1 mol dm^{-3} Bu_4NBF_4 was contained. The scan rate was 20 mV s^{-1}.

Table 2 Second-order rate constants for reaction of **1** with O_2 at 25 °C

Solvent	Method	$[O_2]$/mol dm^{-3}	k_{obs}/s^{-1}	$k_2/dm^3\ mol^{-1}\ s^{-1}$
DMSO	CV[a]	2.1×10^{-3}	2.63	1.25×10^3
MeCN	CV	8.21×10^{-3}	2.43	2.96×10^2
MeCN	CV	1.72×10^{-3}	0.51	2.94×10^2
MeCN	CL[b]	1.72×10^{-3}	0.32	1.9×10^2
DMF	CV	4.72×10^{-3}	0.452	96
DMF	CL	9.9×10^{-4}	0.090	91
Benzene	UV–VIS[c]	9.1×10^{-3}	3.1×10^{-4}	3.4×10^{-2}

[a] Cyclic voltammetry. [b] Time course of CL intensity. [c] Decay of the absorption of **1**.

$\mathbf{3}^{2+}(I^-)_2$ gave a number of by-products other than 2-methyl-1(2*H*)-isoquinolinone **6**. Furthermore, the actual emitter for $\mathbf{2}^{2+}$ or $\mathbf{3}^{2+}$ was not the S_1 state of the isoquinolinone but the excited state of another compound formed *via* energy transfer.[4]

A reaction of $\mathbf{1}^{2+}$ with KO_2 in MeCN also produced a CL emission and gave **4** in a high yield (>99%). A trace amount (<1%) of the intramolecular [2 + 2] cycloadduct of **4** was also detected by ^{1}H NMR spectroscopy. The CL quantum yield was determined to be $(6 \pm 1) \times 10^{-3}$. This value was comparable with that of 9,10-dicyanoanthracene–KO_2 reaction in THF (2×10^{-3}) reported by Breslin and Fox.[9] For direct (not *via* energy transfer to a secondary emitter) CL reactions, Φ_{CL} is expressed as eqn. (1) where Φ_R, Φ_S* and Φ_{FL} are the chemical

$$\Phi_{CL} = \Phi_R\ \Phi_S^*\ \Phi_{FL} \quad (1)$$

reaction yield, fraction of the S_1 state and fluorescence quantum yield of the emitter, respectively. In the present case, because no alternative pathway was observed to compete with the CL process, Φ_R is equal to unity. Using Φ_{FL} value of 0.097 for **4** in aerated MeCN,† eqn. (1) gives Φ_S* of 0.06, which is much higher than that for decomposition of unsubstituted or methyl-substituted 1,2-dioxetanes (3×10^{-6}–2.5×10^{-3}).[10] As for some dioxetanes with an electron-rich substituent, intramolecular CIEEL[11] or a CT[12] mechanism has been proposed,[13] but this process is unlikely to occur for neutral symmetrical dioxetanes. Intermolecularly, aromatic compounds having a low oxidation potential such as **1** (Table 1) could play the role of an activator in CL reactions.[11,12] In the reaction of $\mathbf{1}^{2+}$, however, it was not **1*** but **4*** that emitted light, and therefore, this possibility was ruled out. Under these conditions the CL intensity of $\mathbf{2}^{2+}$ or $\mathbf{3}^{2+}$ was lower than that of $\mathbf{1}^{2+}$. In the case of $\mathbf{2}^{2+}$, the major product was **5** and the intramolecular cycloadduct of **5** was also formed (*ca.* 10% yield). Since the cycloadducts had been obtained by triplet-sensitised photolysis of **4** or **5**,[4] these products may be formed from the chemically generated T_1 state in the CL reaction. On addition of KO_2 in MeCN, $\mathbf{3}^{2+}(I^-)_2$ gave a complex mixture including **6**.

Reaction mechanism and kinetics

We focus on the CL reaction of $\mathbf{1}^{2+}$ and its reduced species in aprotic solvents for the following reasons: (*i*) the chemical yield of **4** was high, (*ii*) the emitter is the S_1 state of **4** which is formed directly *via* thermal decomposition of the dioxetane, (*iii*), $O_2^{\bullet-}$ is stable against disproportionation on the timescales of our experiments (< 10^2 s) in aprotic media, (*iv*) the system does not contain OH^- or MeO^-, which may cause nucleophilic attack on $\mathbf{1}^{2+}$ and/or $\mathbf{1}^{\bullet+}$. In order to get information on the rate determining step in the reaction of **1** with O_2, the kinetics of CL emission and disappearance of **1** were examined at 25 °C under air or an oxygen atmosphere. Time courses of the CL intensity were recorded at 390 nm in DMF and MeCN. After a time lag of a few seconds, the decay curve could be fitted to a single exponential function. The time lag may be an artifact because the absorption and CL spectra partially overlapped. Table 2 lists the observed rate constants of the disappearance of **1** under pseudo-first-order conditions, k_{obs}. As for the electrochemical studies, the k_{obs} values were determined from the cathodic peak potentials of the $\mathbf{1}^{\bullet+}/\mathbf{1}$ couple at various scan rates, using a working curve for an EC reaction investigated by Nicholson and Shain.[14] The presence of O_2 did not affect the redox wave of the $\mathbf{1}^{2+}/\mathbf{1}^{\bullet+}$ couple. The reaction rate of the disappearance of **1** was found to be first order with respect to the concentration of O_2, and therefore it is expressed by eqn. (2).

$$-d[\mathbf{1}]/dt = k_2[\mathbf{1}][O_2] \quad (2)$$

Using the reported data for solubility of O_2,[15] bimolecular rate constants k_2 were obtained. The k_2 values determined by spectrophotometric and electrochemical methods were in agreement with each other. In nonpolar solvents such as benzene, the disappearance of **1** was much slower than that in polar solvents, suggesting that the **1**–O_2 reaction should involve a polar intermediate in the rate determining step. As is seen in Table 2, however, the k_2 value in DMSO was more than ten times larger than that in DMF in spite of a similar polarity. Inspection of Tables 1 and 2 reveals that the rate constant k_2 correlated with the free energy change for an electron-transfer (ET) from **1** to O_2, although this ET process was endothermic (ΔG° = 29–42.5 kJ mol^{-1}) in all the solvents studied. The more negative the redox potential, the larger the k_2 value was observed.

Eberlein and Bruice investigated autoxidation of 1,10-ethano-5-ethyl-1,5-dihydrolumiflavin (Fl_{red}) in an aqueous solution and proposed that Fl_{red} transferred an electron to O_2 to yield a radical pair $\{Fl^{\bullet+} \cdots O_2^{\bullet-}\}$ followed by radical coupling leading to a zwitterionic intermediate, although this ET reaction was rather endothermic (ΔG° = 57 kJ mol^{-1}).[16] Nanni *et al.* reported that radical cation of methyl viologen (MV^{2+}) reacted with O_2 in a DMF solution.[17,18] In the presence of a large excess of $MV^{\bullet+}$, O_2 was reduced *via* one ET from $MV^{\bullet+}$, and the resultant $O_2^{\bullet-}$ reacted with another molecule of $MV^{\bullet+}$ to give a radical-coupling product. They suggested that the coupling would be fast, although $O_2^{\bullet-}$ can reduce $MV^{\bullet+}$ to MV.[18] In order to examine whether $\mathbf{1}^{\bullet+}$ reacts with $O_2^{\bullet-}$ to give **4*** in aprotic solvents or not, KO_2 was added to an MeCN solution of $\mathbf{1}^{\bullet+}$. A bright emission was instantaneously observed, and the CL spectrum coincided with the fluorescence spectrum of **4**. From these facts, a possible reaction mechanism is proposed. One ET from **1** to O_2 yields a radical ion pair $\{\mathbf{1}^{\bullet+} \cdots O_2^{\bullet-}\}$, and the coupling of the component radicals gives a 1,2-dioxetane *via* a zwitterion intermediate (Scheme 2). Under con-

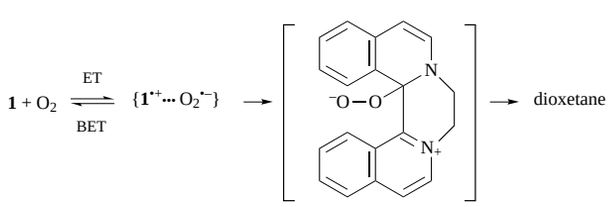

Scheme 2

† The CL quantum yield was also determined under air.

ditions used for the **1**–O_2 reaction, a large excess of O_2 exists in the solution. If $\mathbf{1}^{\bullet+}$ were trapped by O_2, a peroxyl radical would be formed, which might cause a radical chain reaction. In fact, the second-order rate constant for the reaction of $\mathbf{1}^{\bullet+}$ with O_2 was 1.5×10^{-2} dm^3 mol^{-1} s^{-1} in MeCN at 25 °C, which was negligible compared with the k_2 value of the **1**–O_2 reaction. This low reactivity of $\mathbf{1}^{\bullet+}$ to O_2 was consistent with the result that the redox wave of the $\mathbf{1}^{2+}/\mathbf{1}^{\bullet+}$ couple was not affected by the presence of O_2. In the reaction of $\mathbf{1}^{2+}$ with an excess amount of KO_2, $\mathbf{1}^{2+}$ is readily reduced with $O_2^{\bullet-}$ and the resultant $\mathbf{1}^{\bullet+}$ combines with another molecule of $O_2^{\bullet-}$ as shown in eqn. (3).

$$\mathbf{1}^{2+} + O_2^{\bullet-} \longrightarrow \mathbf{1}^{\bullet+} + O_2 \qquad (3a)$$

$$\mathbf{1}^{\bullet+} + O_2^{\bullet-} \longrightarrow \text{Dioxetane} \qquad (3b)$$

Further reduction of $\mathbf{1}^{\bullet+}$ with $O_2^{\bullet-}$ [eqn. (4)] can also take

$$\mathbf{1}^{\bullet+} + O_2^{\bullet-} \longrightarrow \mathbf{1} + O_2 \qquad (4)$$

place, but **1** thus formed will react with O_2. In the mechanism shown in Scheme 2, the coupling of $\mathbf{1}^{\bullet+}$ and $O_2^{\bullet-}$ should be fast enough to compete with back electron-transfer (BET). It may be possible if the coupling reaction takes place within the geminate radical ion pair $\{\mathbf{1}^{\bullet+} \cdots O_2^{\bullet-}\}$. Recently Yamaguchi and co-workers investigated the mechanism of autoxidation of phenol and indole derivatives.[19] According to their calculations, one ET from phenolate anion to O_2 can occur with assistance by hydrogen bonding between $O_2^{\bullet-}$ and protic solvents, while in aprotic media formation of a ^{3}CT complex followed by spin inversion to a ^{1}CT state is energetically favourable. If a similar CT complex is formed from **1** and O_2, then Scheme 2 should be modified as shown in Scheme 3. Formation of a C–O bond

$$\mathbf{1} + O_2 \rightleftharpoons {}^3\{\mathbf{1}^{\delta+} \cdots O_2^{\delta-}\} \longrightarrow {}^1\{\mathbf{1}^{\delta+} \cdots O_2^{\delta-}\} \longrightarrow [\text{zwitter ion or biradical}] \longrightarrow \text{dioxetane}$$

Scheme 3

within the singlet CT complex will give a zwitterion (or less likely biradical) intermediate,[20] which will then cyclise to a 1,2-dioxetane.

Rate constants for reaction of **2** or **3** with O_2 could not be determined because of experimental difficulties. The absorption spectrum of the starting olefin and the CL spectrum overlapped with each other. Electrochemical methods seemed to be better, but the second reduction potential of $\mathbf{2}^{2+}$ or $\mathbf{3}^{2+}$ was close to that of O_2 in MeCN or DMSO. Qualitative analyses of the cyclic voltammograms in aerated DMF indicated that the disappearance of **2** or **3** was faster than that of **1**. As is seen in Table 1, the free energy change for the ET process from **2** or **3** to O_2 was smaller than that from **1**, and this correlation supported the proposed mechanism involving an ET or CT process. Although a single ET cannot be discriminated from a partial CT for BIQ–O_2 system, the relatively sharp dependence of k_2 on $\Delta G°$ (ET) suggests a significant contribution of a state where an electron has been transferred to O_2 from the olefin.

In solvents with low polarity, oxygenation of **1** was rather slow. On addition of a drop of MeOH to the solution, however, a bright CL emission was instantaneously observed. Previously, Heller *et al*. reported that an alcoholic solvent worked as catalyst for oxygenation of electron-rich olefins such as **1** and tetrakis(dimethylamino)ethylene.[3,21] A plausible reaction pathway for this catalytic process is proposed. In the presence of MeOH, oxygen will accept one electron from **1** more easily, since superoxide is stabilised by hydrogen bonding with MeOH or by protonation to give a hydroperoxyl radical ·OOH. Such a reactive radical thus formed rapidly combined with $\mathbf{1}^{\bullet+}$, and eventually **4*** is formed *via* the 1,2-dioxetane.

Redox behaviour of BQ^{2+} salts

If an ET or CT process generally takes place between an electron-rich olefin and molecular oxygen, a substrate with a redox potential similar to that of BIQ may undergo the same type of oxygenation reaction. We have synthesized 2,2′-biquinolinium (BQ^{2+}) salts , which have a closely related structure with BIQ^{2+}, and investigated their redox properties and CL reactions.

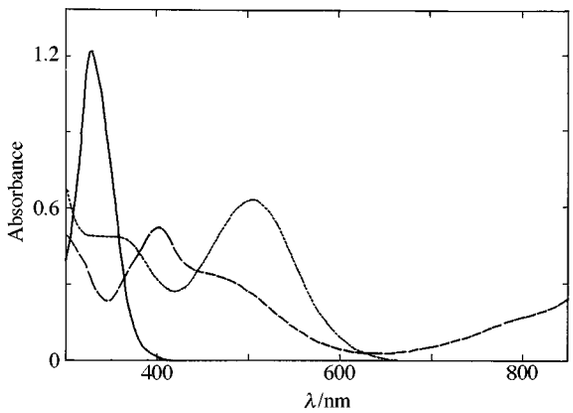

Fig. 1 Absorption spectra of $\mathbf{7a}^{2+}$ (——), $\mathbf{7a}^{\bullet+}$ (– – –) and **7a** (· · ·) in MeCN. $[\mathbf{7a}^{2+}] = 5.9 \times 10^{-5}$ mol dm^{-3}.

Cyclic voltammograms of $\mathbf{7a}^{2+}$–$\mathbf{7c}^{2+}$ in MeCN showed two reversible one-electron redox waves in each case. The peak separation between cathodic and anodic scans was 55–70 mV at the scan rate of 10–100 mVs^{-1}. As is shown in Table 1, the redox potential of $BQ^{\bullet+}/BQ$ is a little less negative than that of $\mathbf{1}^{\bullet+}/\mathbf{1}$. In a solvent having a high donor number, the first reduction potential of BQ^{2+} is shifted towards the more negative value. On the other hand, the second redox potential is largely unaffected, and as a result only one redox wave is observed in DMSO. Substitution by methyl groups shifted reduction potentials to the negative direction, and a 4-methyl group had a larger effect than one at the 6-position. Because introduction of a methyl group at the 4- or 6-position does not cause further steric interaction between the two quinoline rings, the observed effect is attributed to the electronic nature of the substituent. PM3 calculations[22] for $\mathbf{7a}^{\bullet+}$ indicated that the spin density at the 4-position is higher than that of the other CH carbons (*vide infra*), and therefore, an electron-donating substituent at the 4-position seems to make the radical less unstable.

Reduction of BQ^{2+} with Na/Hg was carried out using the same procedure as that reported for BIQ^{2+}.[4] Variation of the absorption spectra on reduction of $\mathbf{7a}^{2+}$ in MeCN is shown in Fig. 1. A transient orange species with a structured absorption band in 400–580 nm showed an EPR signal, and the signal disappeared on further reduction to a reddish violet form. These results confirmed that $\mathbf{7a}^{2+}$ was reduced to radical cation $\mathbf{7a}^{\bullet+}$ and then to diamagnetic neutral species **7a** (Scheme 4).

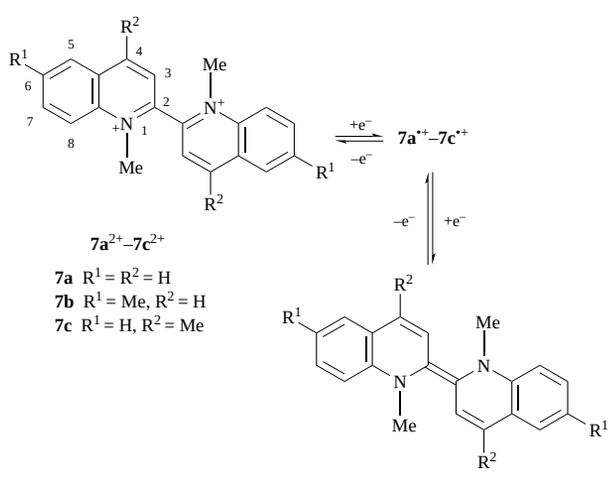

Scheme 4

Table 3 Absorption maxima (nm) of BQ^{2+}, $BQ^{\bullet+}$ and BQ in MeCN

	BQ^{2+}	$BQ^{\bullet+}$ [a]	BQ
7a	329	404	506
7b	336	406	516
7c	327	396	505

[a] The longest wave absorption of $BQ^{\bullet+}$ was observed in the near IR region.

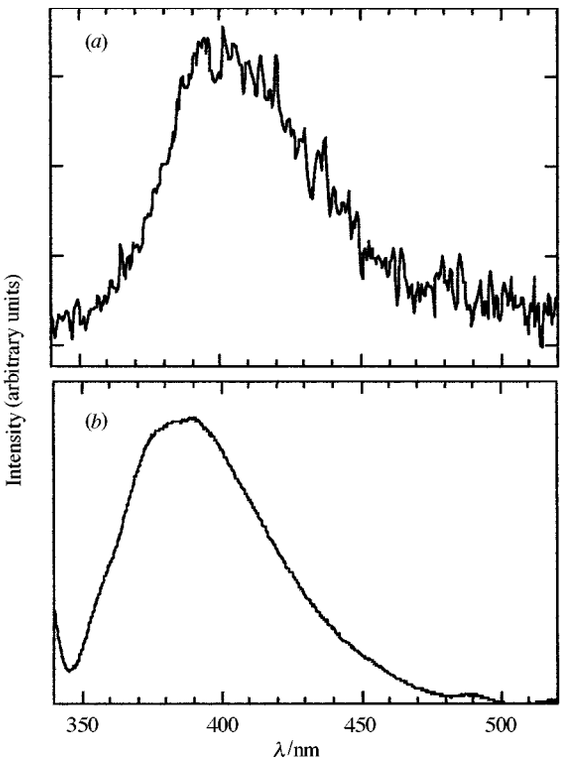

Fig. 2 (*a*) CL spectrum of the reaction of $\mathbf{7a}^{2+}(PF_6^-)_2$ with KO_2 in MeCN–DMSO. (*b*) Fluorescence spectrum of **8a** in MeCN (excitation at 332 nm).

The absorption spectrum of **7a** in benzene (λ_{max} 505 nm) was quite similar to that recorded in MeCN. As is seen in Table 3, substitution by methyl groups caused only a small shift of the absorption maxima. In the case of the BIQ series studied, the absorption spectra showed a large variation with the bridge on the nitrogen atoms, reflecting the difference in the degree of conjugation between the two isoquinoline rings.[4] It is noteworthy that BQ shows a longer wavelength absorption than BIQ (400–450 nm), which is probably due to the more planar structure of the former π system. The ^{1}H NMR spectrum of **7a** in C_6D_6 showed that it was a single isomer, probably (*E*)-form. PM3 calculations showed that (*E*)-**7a** with C_i symmetry has a lower energy than the (*Z*)-isomer. In the case of olefin **3**, a mixture of (*E*)- and (*Z*)-forms was obtained on reduction of $\mathbf{3}^{2+}(I^-)_2$ with aqueous $Na_2S_2O_4$.[4] In the PM3 optimized structure of either isomer, the central C=C double bond is highly twisted. The torsion angles of N(2)–C(1)–C(1′)–N(2′) are 142 and 34° for the (*E*)- and (*Z*)-forms, respectively.

CL reaction of BQ^{2+} salts

On addition of aqueous H_2O_2–NaOH to an aqueous solution of $\mathbf{7a}^{2+}(MeSO_4^-)_2$, a bluish violet CL was observed. The major product of this reaction was identified to be 1-methyl-2(1*H*)-quinolinone (**8a**) based on a comparison of the ^{1}H NMR spectrum with that of the authentic sample. At high pH $\mathbf{7a}^{2+}$ was unstable.[23] On addition of an excess amount of NaOD to a solution of $\mathbf{7a}^{2+}(MeSO_4^-)_2$ in D_2O, the variation of the ^{1}H NMR spectrum showed that $\mathbf{7a}^{2+}$ was completely transformed to a new compound. Although the structure of this product

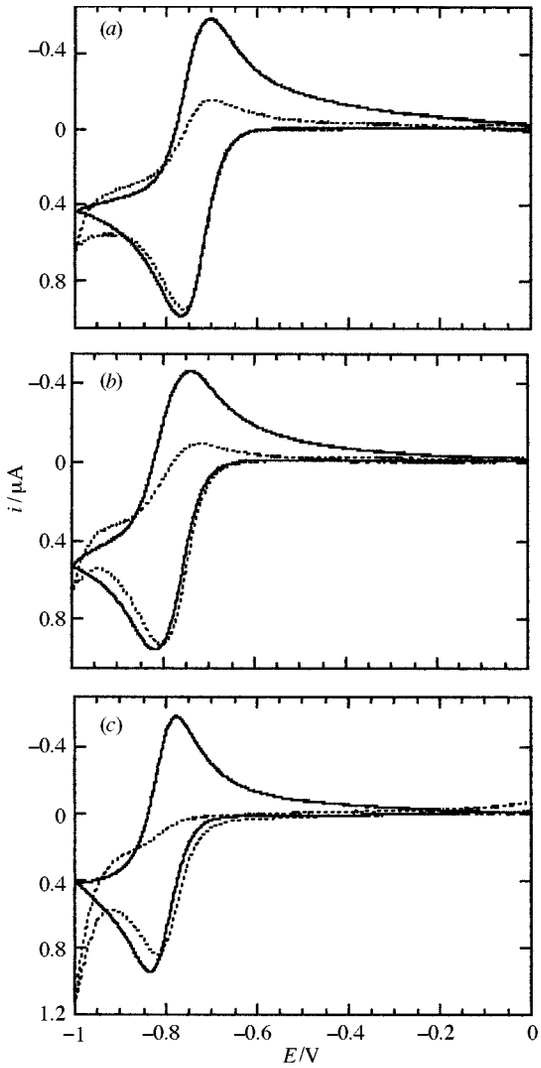

Fig. 3 Cyclic voltammograms of (*a*) $\mathbf{7a}^{2+}$, (*b*) $\mathbf{7b}^{2+}$ and (*c*) $\mathbf{7c}^{2+}$ in DMSO at 25 °C at a scan rate of 30 mV s^{-1}. —— : under Ar. – – – : under O_2. $[\mathbf{7}^{2+}] = ca.\ 1.6 \times 10^{-4}$ mol dm^{-3}.

was not determined, the ^{1}H and ^{13}C NMR spectra indicated inequivalence of the two quinoline groups, and it was likely to be an OH^- adduct. Addition of aqueous H_2O_2 to this product brought about no CL, indicating that it was not involved in the CL reaction. Reaction of $\mathbf{7a}^{2+}$ with KO_2 or **7a** with O_2 in MeCN also gave **8a** with light emission. Fig. 2(*a*) shows the CL spectrum recorded on addition of KO_2 to a solution of $\mathbf{7a}^{2+}(PF_6^-)_2$ in MeCN. The spectrum was similar to the fluorescence of **8a** in MeCN [Fig. 2(*b*)], and the emitter of this CL was determined to be the singlet excited state of **8a**. Reaction of **7b** and **7c** with O_2 in MeCN showed blue emission and gave the corresponding 1-methyl-2(1*H*)-quinolinones **8b** and **8c**, respectively as the major product. Compared with the reaction of **1** with O_2, oxygenation of **7a** under the same conditions was slower, and the CL efficiency (Φ_{CL}) was lower by two orders of magnitude. The lower Φ_{CL} value is partially attributed to the lower fluorescence quantum yield of **8a** (0.017). Furthermore, in the CL reactions of BQ–O_2 or BQ^{2+}–KO_2, several unidentified minor products were also formed, which also resulted in a decrease in the CL efficiency.

In the BQ series studied, the steric interaction in the formation of the corresponding dioxetane is almost the same among the three compounds, and therefore it seems suitable to investigate effects on the reactivity of O_2 stemming from the redox potentials and/or the electronic structure of BQ and $BQ^{\bullet+}$. As for the **7a**–O_2 reaction in MeCN, because the CL intensity was very low, the disappearance of the absorption due to **7a** was

monitored at 505 nm. The absorbance *vs*. time curve was fitted to first-order kinetics to give a rate constant of $(1.2 \pm 0.1) \times 10^{-2}$ s^{-1}, and using the concentration of O_2 (1.72×10^{-3} mol dm^{-3}),[15] a k_2 value of 7.0 ± 0.6 dm^3 mol^{-1} s^{-1} was obtained at 25 °C. For **7b** and **7c**, the CL intensity per unit time was higher than that of **7a**, and the decay was faster under the same conditions. The observed CL intensity *vs*. time curve could be fitted to an exponential decay with a second-order rate constant of 26 dm^3 mol^{-1} s^{-1} (for **7b**) or 25 dm^3 mol^{-1} s^{-1} (for **7c**). The obtained rate constants for autoxidation of **7a**–**7c** were lower than that of **1**.

Electrochemical methods were also attempted. In MeCN, the two reduction peaks partially overlapped and the $\mathbf{7}^{2+}/\mathbf{7}^{\bullet+}$ redox wave was affected by the presence of O_2, indicating that $\mathbf{7}^{\bullet+}$ also reacted with O_2 on a 1 s timescale. Fig. 3 shows cyclic voltammograms of $\mathbf{7a}^{2+}$–$\mathbf{7c}^{2+}$ in deaerated or O_2-saturated DMSO at a scan rate of 30 mV s^{-1}. Although only one redox wave was observed in each case, the ratio of the cathodic and the anodic peak currents was almost unity under anaerobic conditions, indicating that both of the two redox reactions were electrochemically reversible. In O_2-saturated solution, the reoxidation peak was significantly diminished (for **7a** and **7b**) or disappeared (for **7c**), and the order of reaction rate was **7c** > **7b** > **7a**. Thus the relative reactivity of **7a**–**7c** to oxygenation clearly correlates with free energy change for an ET from these olefins to O_2 (Table 1). From these results and an analogy with the BIQ–O_2 system, reaction of BQ with O_2 is considered to be initiated by an ET process or formation of a CT complex, and coupling at the 2-position leads to a zwitterion intermediate, which eventually cyclises to a 1,2-dioxetane. Thermal decomposition of the dioxetane will generate the S_1 state of **8** as the emitter (Scheme 5).

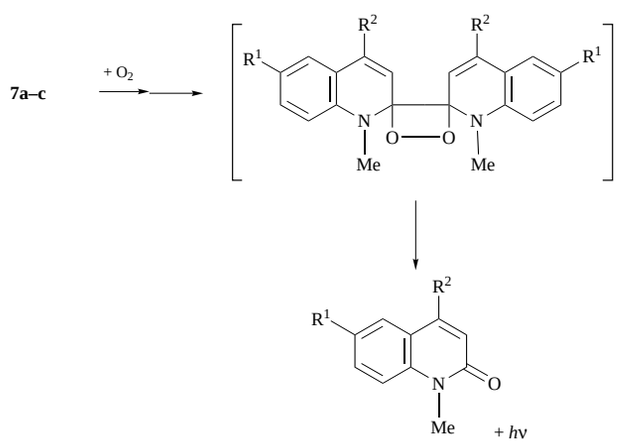

8a–c

8a $R^1 = R^2 = H$
8b $R^1 = Me$, $R^2 = H$
8c $R^1 = H$, $R^2 = Me$

Scheme 5

Electronic structure of radical cations

As was described above, the chemical yield of the emitter was not so high except for the **1**–O_2 reaction. In alkaline aqueous solution, nucleophilic attack of OH^- or OOH^- to BIQ^{2+} or BQ^{2+} caused undesired side reactions. On the other hand, in the coupling between $BIQ^{\bullet+}$ or $BQ^{\bullet+}$ and $O_2^{\bullet-}$, regioselectivity of radical attack is important. If C–O bond formation occurs exclusively at the 1-position in $BIQ^{\bullet+}$ (or the 2-position in $BQ^{\bullet+}$), the 1,2-dioxetane will be formed quantitatively, resulting in a high yield of the emitter. Alternatively, $O_2^{\bullet-}$ may attack another position with a high spin density to give another product. In this regard the spin density distributions in $\mathbf{1}^{\bullet+}$, $\mathbf{3}^{\bullet+}$ and $\mathbf{7a}^{\bullet+}$ were examined by means of EPR, NMR and semiempirical MO calculations.

The EPR spectrum of $\mathbf{1}^{\bullet+}$ in MeCN with a modulation width of 1 G consisted of 11 lines with an averaged line separation of 4.1 G, which was similar to that recorded in MeOH.[1] At a small modulation (0.05 G) about 150 lines were observed over 45 G, but low- or high-field wings could not be analysed due to a poor S/N ratio, while in the central part several signals seemed to overlap owing to coincidental degeneracy. Determination of the hyperfine coupling constants of nitrogen and each proton seemed difficult from the EPR spectra alone. The relative magnitudes of proton hyperfine couplings can be estimated by NMR line broadening resulting from an electron exchange between related diamagnetic and paramagnetic species.[24] According to Johnson's treatment using density matrix formalism,[25] the linewidth contribution from the self-exchange is given by eqn. (5) where k is the second-order rate constant, a is

$$\Delta T_2^{-1} = k[P]/(1 + 4k^2[D]^2/a^2) \quad (5)$$

the hyperfine coupling constant in angular frequency units, [D] and [P] are the concentrations of the diamagnetic and paramagnetic partners. In fast-exchange limit or intermediate cases, the line becomes broader with an increase in the a value. In the ^{1}H NMR spectrum of $\mathbf{1}^{2+}$ in the presence of a small amount of $\mathbf{1}^{\bullet+}$, the observed line broadening showed that hyperfine coupling constants $|a^H|$ increase in the order 8-H < 6-H ~ 5-H < 3-H < 7-H < NCH_2 < 4-H. As for the NCH_2 protons, there are two nonequivalent sets of positions, pseudo-axial and pseudo-equatorial, which are interconvertible. In the absence of electron exchange, the NMR signals due to the methylene protons were observed as an AA′BB′ system even at 70 °C, indicating that the inversion of the ethylene bridge was frozen on the NMR timescale. It seems reasonable to assume that the inversion rate in $\mathbf{1}^{\bullet+}$ should be similar or a little larger than that in $\mathbf{1}^{2+}$ from an analogy with the cases of the 9,10-dihydrophenanthrene radical anion[26] and the diquat radical cation.[27] Accordingly, the signals due to the axial and equatorial protons should show not an averaged but respective ΔT_2^{-1} values. Unfortunately, because of small differences in the chemical shift and a large ^{1}H–^{1}H coupling constant, these two signals overlapped with each other, and contribution to the linewidth from each signal could not be separated. In order to avoid the complexity resulting from the ^{1}H–^{1}H coupling, the ^{2}H NMR spectrum of [$^2H_4$]ethylene-bridged compound [$^2H_4$]$\mathbf{1}^{2+}$ was recorded in the presence of [$^2H_4$]$\mathbf{1}^{\bullet+}$. The ΔT_2^{-1} values for the axial and equatorial deuterons were the same within experimental error, indicating that either position showed a similar hyperfine coupling. The EPR spectrum of [$^2H_4$]$\mathbf{1}^{\bullet+}$ consisted of seven lines with an averaged separation of 4.4 G. Such spectral change on deuterium substitution can be explained by coupling with four protons having an equal a^H value of 4.0–4.3 G. The angular dependence of a hyperfine coupling constant for a β-proton is most simply expressed as $a_\beta^H = B\cos^2\theta$ where θ is the angle between the p_z orbital on the nitrogen and the C_β–H bond.[27] The θ values for axial and equatorial protons in a PM3-optimized structure for $\mathbf{1}^{\bullet+}$ are 30 and 116°, respectively, which predicts an $a_\beta^{ax}/a_\beta^{eq}$ ratio of 3.9:1. A discrepancy in the results of the NMR experiments ($a_\beta^{ax}/a_\beta^{eq} = ca.$ 1) cannot be explained at the present stage. A large twisting angle between the two isoquinoline rings (37°) might affect the hyperfine coupling constants, and the above formula for the angular dependence may be over simplified.

Similar NMR experiments were attempted for $\mathbf{3}^{2+}$ and $\mathbf{7a}^{2+}$. In the case of $\mathbf{3}^{2+}$, the signals due to 8-H and 6-H were less broadened than the other signals, indicating that the a^H values at these positions were small. However, the linewidths of all the other signals were almost the same. As for $\mathbf{7a}^{2+}$, all the signals were equally broadened. This result means that the self exchange for $\mathbf{7a}^{2+}/\mathbf{7a}^{\bullet+}$ was so slow that the situation fell in a slow-exchange limit even at a relatively high concentration of the diamagnetic partner (0.06 mol dm^{-3}).

Table 4 Calculated spin densities for the most stable conformer of radical cations[a]

Compd.	C-1 or C-2[b]	N	C-3	C-4	C-5	C-6	C-7	C-8
$\mathbf{1}^{\bullet+}$	0.149	0.152	0.013	0.062	0.006	0.021	0.012	0.013
$\mathbf{3}^{\bullet+}$	0.161	0.151	0.009	0.061	0.009	0.022	0.013	0.018
$\mathbf{7a}^{\bullet+}$	0.146	0.163	0.019	0.063	0.007	0.021	0.011	0.015

[a] The structure was optimized by the ROHF (for $\mathbf{1}^{\bullet+}$) or UHF (for $\mathbf{3}^{\bullet+}$ and $\mathbf{7a}^{\bullet+}$) method using PM3 parameters. [b] C-1 for $\mathbf{1}^{\bullet+}$ and $\mathbf{3}^{\bullet+}$, C-2 for $\mathbf{7a}^{\bullet+}$

In order to investigate the structure of the radical cations, PM3 calculations were carried out for $\mathbf{1}^{\bullet+}$, $\mathbf{3}^{\bullet+}$ and $\mathbf{7a}^{\bullet+}$. In the optimized structure, the central C–C bond distance was shortened by 0.04–0.05 Å compared with that of the corresponding dication. In the case of $\mathbf{1}^{\bullet+}$, other structural parameters including the torsion angle of N(2)–C(1)–C(1′)–N(2′) were similar to the corresponding values in $\mathbf{1}^{2+}$. On the other hand, $\mathbf{3}^{\bullet+}$ and $\mathbf{7a}^{\bullet+}$ showed two local minima with different twisting angles. In the conformer with the lowest energy, the torsion angle was 115 and 140° for $\mathbf{3}^{\bullet+}$ and $\mathbf{7a}^{\bullet+}$, respectively, while the dications showed a single minimum at *ca*. 100° along the rotation of the central bond. The large geometry change on reduction from $\mathbf{7a}^{2+}$ to $\mathbf{7a}^{\bullet+}$ probably caused a high intramolecular reorganization energy, and the self-exchange rate decreased, as was mentioned above. Shortening of the central bond and an increase in coplanarity of the two aromatic rings suggest that conjugation between the two halves of the molecule should stabilise the radical.

Table 4 lists calculated RHF spin densities of the most stable conformer for each radical. The three radicals showed a similar spin density distribution. The unpaired electron delocalises on the whole molecule, but the C-1 (or C-2 in $\mathbf{7a}^{\bullet+}$) has the highest spin density among the carbon atoms, which is consistent with the result that $O_2^{\bullet-}$ attacked this position of the radical cation. The calculated spin densities for $\mathbf{1}^{\bullet+}$ predicts that the hyperfine coupling will increase in the order 5-H < 7-H < 8-H ~ 3-H < 6-H < 4-H. Although this order is slightly different from the result of NMR experiments, the spin density at the 4,4′-position has been proved to be high. If the $O_2^{\bullet-}$ attacks this position, a dioxetane bridged at the 3,4-positions will be formed and the cleavage of its four-membered ring will result in destruction of the isoquinoline ring. As for the autoxidation of BIQ and BQ, factors controlling the chemical yield of the emitter as well as an origin of the inconsistency between experimental and calculated spin densities is still an open question. Further investigation of the electronic structures of these radicals is in progress.

Conclusion

Autoxidation of electron-rich olefins BIQ and BQ is not a radical chain process but a bimolecular reaction of the substrate and triplet dioxygen. In polar aprotic solvents the reaction rate correlated with the free energy change for an ET from the substrate to $^3O_2$, while in non-polar solvents the reaction is very slow. These results strongly suggest that the reaction should be initiated by an ET or CT process to give a radical ion pair, and then intersystem crossing takes place from the triplet to the singlet state followed by formation of a C–O bond. All the olefins studied produce light emission through the same type of reaction pathway, but the CL efficiency and the chemical yield of the emitter varies from compound to compound, probably reflecting the difference in the electronic structure and the steric interactions during bond formation.

Experimental

Apparatus

Absorption and fluorescence spectra were recorded on a Shimadzu UV2200 spectrophotometer and a Shimadzu RF510 fluorophotometer equipped with a quantum counter, respectively. Fluorescence quantum yields were determined at 25 °C using anthracene in EtOH as standard. The CL spectra were recorded with a Hamamatsu Photonics PMA-10 spectrophotometric multichannel analyser. ^{1}H (270 or 400 MHz) and ^{2}H (61.4 MHz) were obtained with a JEOL JNM-GSX400 or JNM-GSX270 spectrophotometer. *J* values are given in Hz. The residual protons in the solvent or sodium 2,2-dimethyl-2-silapentane-5-sulfonate (in D_2O) were used as internal reference. EPR spectra (X-band) were recorded on a JEOL JES-FE2XG spectrometer equipped with a temperature control unit ES-DVT1 with 100 kHz modulation. IR spectra were obtained with a Perkin-Elmer Spectrum 2000 FTIR spectrometer as KBr disks. Melting points were determined on a Yanaco micro apparatus and are uncorrected.

Materials

Solvents used for the measurements of the fluorescence spectra were of spectroscopic grade. DMSO and DMF were distilled from CaH_2 under reduced pressure just before use. *tert*-Butyl alcohol was dried over activated molecular sieves 4 Å. Potassium *tert*-butoxide was dried *in vacuo* at room temp. before use. CD_3CN (Isotec, 99.8% D) was dried over molecular sieves 3 Å and stored under vacuum. Anthracene was recrystallised from EtOH. The purity of luminol (Wako) was checked with the UV spectrum and used without further purification. Other reagents were used as received.

2,2′-Ethylene-1,1′-biisoquinolinium hexafluorophosphate $\mathbf{1}^{2+}(\mathbf{PF_6^-})_2$. To an aqueous solution of $\mathbf{1}^{2+}(Br^-)_2$ (189 mg, 0.42 mmol), aq. KPF_6 (200 mg, 1.09 mmol) was added. The resultant yellow precipitate was filtered, washed with water and recrystallised from aqueous MeCN to give $\mathbf{1}^{2+}(PF_6^-)_2$ as fine yellow crystals (124 mg) [Found: C, 42.3; H, 2.8; N, 4.95. $C_{20}H_{16}N_2(PF_6)_2$ requires C, 41.8; H, 2.8; N, 4.9%]. δ_H (CD_3CN) 5.19 (2H, m, NCH_2 ax), 5.30 (2H, m, NCH_2 eq), 7.83 (2H, d, *J* 8.8, 5,5′-H), 7.92 (2H, ddd, *J* 8.8, 7 and 1.2, 6,6′-H), 8.33 (2H, ddd, *J* 8.5, 7 and 1.2, 7,7′-H), 8.51 (2H, d, *J* 8.5, 8,8′-H), 8.89 (2H, d, *J* 6.5, 4,4′-H) and 8.91 (2H, d, *J* 6.5, 3,3′-H).

1,1′-Dimethyl-2,2′-biquinolinium hexafluorophosphate $\mathbf{7a}^{2+}(\mathbf{PF_6^-})_2$. To an aqueous solution $\mathbf{7a}^{2+}(MeSO_4^-)_2$,[23] aq. KPF_6 (2.5 equiv.) was added. The resultant white precipitate was filtered, washed with water and dried. Recrystallisation from EtOH–MeCN gave faint pink, plate-like crystals [Found: C, 42.15; H, 3.3; N, 5.8. $C_{20}H_{18}N_2(PF_6)_2{\cdot}0.5(CH_3CN)$ requires C, 42.3; H, 3.3; N, 5.9%]; ν_{max}/cm^{-1} 3096, 1627, 1590, 1521, 1442, 1392, 1351, 842, 779, 755 and 559; δ_H(CD_3CN) 4.41 (6H, s, Me), 8.21 (2H, d, *J* 8.5, 3,3′-H), 8.25 (2H, t, *J* 8, 6,6′-H), 8.51 (2H, ddd, *J* 8, 7 and 1.5, 7,7′-H), 8.57 (2H, d, *J* 8, 5,5′-H), 8.59 (2H, d, *J* 7, 8,8′-H) and 9.43 (2H, d, *J* 8.5, 4,4′-H).

1,1′,6,6′-Tetramethyl-2,2′-biquinolinium hexafluorophosphate $\mathbf{7b}^{2+}(\mathbf{PF_6^-})_2$. The corresponding biquinoline was prepared by the methods of Tiecco *et al.*[28] A DMF solution (10 cm^3) of $NiCl_2{\cdot}6H_2O$ (547 mg, 2.3 mmol) and triphenylphosphine (2.41 g, 9.2 mmol) was stirred under nitrogen at 50 °C, and zinc powder (290 mg, 4.4 mmol) was added to the solution. To the resultant reddish brown solution, a DMF solution (5 cm^3) of 2-chloro-6-methylquinoline[29] (350 mg, 2.0 mmol) was added dropwise. The mixture was stirred at 50 °C for 3 h under nitrogen, cooled, poured into 5% aq. NH_3 (70 cm^3) and extracted with $CHCl_3$. The organic layer was washed with water, dried over Na_2SO_4 and concentrated. The resultant precipitate was filtered and recrystallised from $CHCl_3$ to give 6,6′-dimethyl-2,2′-biquinoline as fine, pale-yellow needles (176 mg, 43%). Mp 260–261 °C; δ_H($CDCl_3$) 2.57 (3H, s, Me), 7.58 (1H, dd, *J* 8.5 and 1.7), 7.64 (1H, br s), 8.11 (1H, d, *J* 8.5), 8.22 (1H, d, *J* 8.5) and 8.77 (1H, d, *J* 8.5).

A mixture of 6,6′-dimethyl-2,2′-biquinoline (80 mg, 0.28 mmol) and dimethylsulfate (1.5 cm^3) was heated to 170 °C for 80 min. The mixture was cooled, water and diethyl ether were

added and the aqueous layer was separated, to which aq. KPF_6 (186 mg, 1.0 mmol) was added. The resultant white precipitate was filtered and recrystallised from aqueous MeCN to give **7b**$^{2+}(PF_6^-)_2$ as pale-yellow plates (106 mg, 59%) [Found: C, 45.3; H, 3.8; N, 6.3. $C_{22}H_{22}N_2(PF_6)_2\cdot(CH_3CN)$ requires C, 44.7; H, 3.9; N, 6.5%]. ν_{max}/cm^{-1} 3095, 1629, 1589, 1513, 1401, 1351, 821, 715 and 559; $\delta_H(CD_3CN)$ 2.73 (6H, s, 6,6′-Me), 4.35 (6H, s, 1,1′-Me), 8.12 (2H, d, *J* 8.5, 3,3′-H), 8.3 (4H, m), 8.44 (2H, d, *J* 9.5) and 9.26 (2H, d, *J* 8.5, 4,4′-H).

1,1′,4,4′-Tetramethyl-2,2′-biquinolinium hexafluorophosphate 7c^{2+}(PF$_6^-$)$_2$. This compound was synthesised from 2-chloro-4-methylquinoline by the same procedure as that for **7b**$^{2+}(PF_6^-)_2$. Pale-violet needles [Found C, 44.7; H, 3.8; N, 6.4. $C_{22}H_{22}N_2(PF_6)_2\cdot(CH_3CN)$ requires C, 44.7; H, 3.9; N, 6.5%]. ν_{max}/cm^{-1} 3090, 1622, 1596, 1522, 1370, 836, 766 and 558; $\delta_H(CD_3CN)$ 3.12 (6H, s, 4,4′-Me), 4.32 (6H, s, 1,1′-Me), 8.02 (2H, s, 3,3′-H), 8.21 (2H, ddd, *J* 8, 7 and 1), 8.43 (2H, ddd, *J* 9, 7 and 1), 8.52 (2H, d, *J* 9) and 8.65 (2H, dd, *J* 8 and 1).

1,6-Dimethyl-2(1*H*)-quinolinone (**8b**)[30] and 1,4-dimethyl-2(1*H*)-quinolinone (**8c**)[31] were synthesised according to the reported procedures. [$^2H_4$]2,2′-Ethylene-1,1′-biisoquinolinium dibromide [$^2H_4$]**1**$^{2+}(Br^-)_2$ was prepared with the same procedures as **1**$^{2+}(Br^-)_2$ using [$^2H_4$]1,2-dibromoethane (99% D).

Cyclic voltammetry

Cyclic voltammograms were obtained on a BAS 100B electrochemical workstation at a scan rate of 10–100 mV s^{-1} using glassy carbon, Pt wire and Ag/Ag^+ as working, counter and reference electrodes, respectively. The sample concentration was *ca*. 2×10^{-4} mol dm^{-3}. Deaeration was done by bubbling with argon until a reduction wave of oxygen was no longer observed (20 min). As for experiments under an oxygen atmosphere, the solution was bubbled with O_2 for 20 min. The background current was corrected. For determination of rate constants, the temperature was maintained at 25 °C by circulation of water to a water jacketed cell from a Shimadzu TB-85 thermostatted bath.

Measurements of relative intensity and quantum yield for CL of BIQ^{2+}

The CL intensity was recorded on a Niti-on lumicounter 1000 connected with a personal computer through an analogue to digital (A/D) converter. In the case of H_2O_2 reaction in alkaline aqueous methanol, a solution of BIQ$^{2+}(X^-)_2$ (1.3×10^{-5} mol dm^{-3}, 300 μl) and 4% aq. hydrogen peroxide (50 μl) were placed in a Pyrex cell which was set in the optical unit of the lumicounter. An aqueous solution of NaOH (0.1 mol dm^{-3}, 50 μl) was added as a starter and the light intensity was collected for 1 min. As for the reaction with KO_2, solid KO_2 (*ca*. 10 mg) was placed in a dried cell, in which a solution of BIQ$^{2+}(X^-)_2$ in MeCN (1×10^{-6} mol dm^{-3}, 150 μl) was injected. CL quantum yields were determined against a luminol standard in DMSO.[32] Five or six runs were performed for each experiment.

CL spectrum of 1$^{\bullet+}$–KO$_2$ reaction. A solution of **1**$^{\bullet+}$ in MeCN was prepared with Na/Hg reduction of **1**$^{2+}(Br^-)_2$ in sealed glassware equipped with a 1 cm quartz cuvette. As soon as the cell was cut off, a small amount of solid KO_2 was added to the solution and the CL spectrum was recorded on the spectrophotometric multichannel analyser.

CL spectrum of 7a^{2+}–KO$_2$ reaction. A solution of **7a**$^{2+}(PF_6^-)_2$ in dry MeCN (1.7×10^{-3} mol dm^{-3}, *ca*. 1.5 cm^3) was placed in a 1 cm quartz cuvette, which was set to the multichannel analyser. Immediately after addition of a solution (0.5 cm^3) of saturated KO_2 in DMSO containing dibenzo-18-crown-6 (0.01 mol dm^{-3}) to the cell, the light emission was accumulated for 5 s.

^{1}H NMR measurement of 7a

A mixture of C_6D_6 (2 cm^3) and a solution of $Na_2S_2O_4$ in phosphate buffer (pH 7.0, 4 cm^3) was put into a test tube stoppered with a rubber septum and bubbled with Ar through a needle for 20 min. To this mixture, **7a**$^{2+}(MeSO_4^-)_2$ (4 mg) in buffer (2 cm^3) was added with a syringe. The mixture was bubbled with Ar at room temp. for 45 min, then the wine-red species was completely transferred to the organic layer and the aqueous phase became almost colourless. A part (*ca*. 0.6 cm^3) of the C_6D_6 solution was transferred to an NMR tube under an Ar atmosphere with a syringe, the tube was stoppered with a Teflon cap and the ^{1}H NMR spectrum was recorded at room temp. δ_H 2.71 (6H, s, Me), 6.03 (2H, d, *J* 10, 3,3′-H), 6.47 (2H, d, *J* 8, 8,8′-H), 6.58 (2H, d, *J* 10, 4,4′-H), 6.82 (2H, t, *J* 7.5), 6.88 (2H, d, *J* 7, 5,5′-H) and 7.08 (2H, t, *J* 7.5).

Identification of the main products in CL reactions of BQ^{2+} salts in MeCN

A solution of BQ$^{2+}(PF_6^-)_2$ ($2–3 \times 10^{-4}$ mol dm^{-3}) was reduced with 0.5% Na/Hg under vacuum by procedures previously reported for reduction of BIQ^{2+}.[4] The progress of the reaction was monitored with UV–VIS spectrometry to ensure complete two-electron reduction. The solution of BQ thus prepared was exposed to air and shaken. After light emission had ceased, the reaction mixture was evaporated under reduced pressure, and the ^{1}H NMR spectrum of the residue was recorded in $CDCl_3$.

In benzene. To a mixture of C_6H_6 (4 cm^3) and $Na_2S_2O_4$ in phosphate buffer (pH 7.0, 3 cm^3), a solution of **7a**$^{2+}(MeSO_4^-)_2$ in the buffer (1.8×10^{-3} mol dm^{-3}, 2 cm^3) was added under an Ar atmosphere. The mixture was continuously bubbled with Ar until the wine-red reduced species moved to the organic phase. The organic layer was transferred to another flask to be exposed to air, and a few drops of MeOH were added as a catalyst for the CL reaction. The mixture was evaporated and the ^{1}H NMR spectrum of the residue was recorded in $CDCl_3$. In the cases of **7b**$^{2+}(PF_6^-)_2$ and **7c**$^{2+}(PF_6^-)_2$, because of the low solubility in water, a suspension of the salt in buffer and C_6H_6 were put into a reaction vessel, to which $Na_2S_2O_4$ in buffer was added under Ar. The mixture was agitated by vigorous bubbling with Ar, and similar work-up procedures were done.

Reaction with KO$_2$. To a solution of BQ$^{2+}(PF_6^-)_2$ in MeCN, a suspension of KO_2 in MeCN was added and the mixture was stirred until the CL had ceased. The supernatant was concentrated and water and $CHCl_3$ were added. The organic layer was separated, dried over Na_2SO_4 and evaporated.

Product analysis of BIQ^{2+}–KO$_2$ reaction

To a solution of BIQ$^{2+}(X^-)_2$ in [$^2H_6$]DMSO, KO_2 was added, and the mixture was stirred until the CL emission ceased. The ^{1}H NMR spectrum of the supernatant was recorded.

Determination of rate constants by emission or UV–VIS spectrometry

A sample solution of **1** in MeCN (2×10^{-4} mol dm^{-3}) or DMF (1×10^{-4} mol dm^{-3}) was prepared in sealed glassware equipped with a 1 cm quartz cuvette with Na/Hg reduction of **1**$^{2+}(Br^-)_2$. Immediately after the glassware was opened and shaken to expose the solution to air, the time course of CL was recorded on a Shimadzu RF510 fluorophotometer at 390 nm (bandwidth 10 nm). During the experiments water at 25 °C was circulated to the cell holder from a Shimadzu TB-85 thermostatted bath. An absorbance or CL intensity *vs.* time curve was fitted to a single exponential decay to obtain the rate constant under pseudo-first-order conditions. Because the absorption of **1** and the CL emission spectra were partially overlapped, the data collected for the initial 5 s were not included for curve fitting. In the cases of **7b** and **7c**, similar procedures were carried out in MeCN.

As for a benzene solution, after **1**$^{2+}$ was reduced to **1** in MeCN using glassware equipped with a vacuum-tight stopcock, the glassware was again connected to the vacuum line to remove the solvent and degassed benzene (3.5 cm^3) was vacuum-transferred onto the residue. The glassware was sealed off from the vacuum line and the reduced species was dissolved in benzene. The cell was opened and connected with a reservoir

containing 1 atm oxygen. After shaking, variation of the UV–VIS spectrum was recorded every 3 min up to 72 min, during which isosbestic points were observed at 350 and 316 nm. From the plot of the logarithm of the absorbance at 440 nm *vs*. time, the rate constant was obtained. The reaction rate of $\mathbf{1}^{\bullet+}$ with O_2 was determined by similar procedures. In the sample preparation, the reduction was stopped when *ca*. 90% of $\mathbf{1}^{2+}$ was converted to $\mathbf{1}^{\bullet+}$ to avoid concomitance of **1**. The absorbance at 500 nm was monitored for 6 h.

EPR spectra of radical cations

A sample solution of a radical cation in MeCN (2×10^{-4}–1×10^{-3} mol dm^{-3}) was prepared by Na/Hg reduction of the corresponding dication under vacuum in sealed glassware equipped with an EPR tube. The variation of the UV–VIS spectrum was monitored, and when *ca*. 90% of the dication was reduced, the solution was transferred to the EPR tube, which was then mounted in an EPR cavity. The signal output for a recorder was fed to an A/D converter, and the spectrum was accumulated 8–32 times using a personal computer.

NMR line broadening experiments for $\mathbf{1}^{2+}$

A solution of $\mathbf{1}^{2+}(Br^-)_2$ (*ca*. 1 mg) in D_2O (0.9 cm^3) was placed in glassware equipped with an NMR tube in which $\mathbf{1}^{2+}(Br^-)_2$ (22 mg) was placed and a branch containing zinc powder. After the solution was degassed by freeze–pump–thaw cycles, a portion of the solution was transferred to the branch to obtain a small amount of $\mathbf{1}^{\bullet+}$, and then the whole solution was transferred to the NMR tube. The tube was sealed off, the solid $\mathbf{1}^{2+}(Br^-)_2$ was completely dissolved (The final concentration of $\mathbf{1}^{2+}$ was *ca*. 0.055 mol dm^{-3}) and NMR spectra were recorded at 22–65 °C. As for ^{2}H NMR measurements, the sample solution was prepared by the same procedures using $[^2H_4]\mathbf{1}^{2+}(Br^-)_2$ and H_2O instead of $\mathbf{1}^{2+}(Br^-)_2$ and D_2O, respectively. The experimental spectra were fitted to the sum of two Lorentzian curves to obtain their linewidths. The frequency difference and linewidths without exchange were determined from the spectrum of a sample containing no radical. The linewidth of a signal due to natural abundance of H*D*O in the solvent showed no difference between samples with and without radical. The ^{1}H NMR signals were assigned based on NOESY experiments (270 MHz, 50 °C) for a sample without a radical. Cross peaks were observed between the pseudo-equatorial methylene protons and 3,3′-H as well as between 4,4′-H and 5,5′-H. δ_H (D_2O, 24 °C, 400 MHz) 5.35 (2H, m, CH_2 ax), 5.54 (2H, m, CH_2 eq), 7.87 (2H, d, *J* 8.2, 5,5′-H), 7.92 (2H, dd, *J* 8.2 and 7, 6,6′-H), 8.33 (2H, dd, *J* 8.2 and 7, 7,7′-H), 8.51 (2H, d, *J* 8.2, 8,8′-H), 8.92 (2H, d, *J* 6.5, 4,4′-H) and 9.11 (2H, d, *J* 6.5, 3,3′-H).

^{1}H NMR line broadening experiments for $\mathbf{3}^{2+}$ and $\mathbf{7a}^{2+}$

In a Pyrex NMR tube, $NaBPh_4$ (7 mg) and $\mathbf{3}^{2+}(PF_6^-)_2$ or $\mathbf{7a}^{2+}(PF_6^-)_2$ were placed and degassed on a vacuum line. CD_3CN (0.8 cm^3) was vacuum-transferred to the tube, which was then sealed off from the vacuum line. The concentration of the dication was *ca*. 0.06 mol dm^{-3}. The sample solution was irradiated with a 500 W xenon lamp for 20 s to obtain a small amount of radical cation *via* photoinduced electron-transfer from tetraphenylborate anion. The ^{1}H NMR spectrum was recorded at room temp.

MO calculations

PM3 calculations were carried out with the program of MOPAC version 6.01.[33] As for $\mathbf{1}^{\bullet+}$ the structure of $\mathbf{1}^{2+}$ determined by X-ray analysis[5] was used as the initial model and structure optimization was performed by ROHF methods with C_2 symmetry. In the cases of $\mathbf{3}^{\bullet+}$ and $\mathbf{7a}^{\bullet+}$, UHF structure optimization was carried out with C_2 symmetry from several initial structures with various torsion angles of N–C–C–N to give two local minima. The unpaired spin density of the more stable conformer was obtained with a single point ROHF calculation using the UHF-optimized geometry. As for neutral species **3** and **7a**, both (*E*)- and (*Z*)-isomers were optimized with C_2 or C_i symmetry.

Acknowledgements

We wish to thank Professor Yuichi Masuda and Ms Haruko Hosoi, Ochanomizu University, for their help with ^{2}H NMR measurements and valuable discussions. We are grateful to Professor Mamoru Ohashi and Dr Takashi Hirano, The University of Electro-Communications, for measuring CL spectra. Thanks are also due to Professor Hajime Nagano, Ochanomizu University, for his discussion and encouragement and to Professor Yutaka Fukuda for his kindness in putting his electrochemical workstation at our disposal. This work was supported by a Grant-in-Aid for Scientific Research from the Ministry of Education, Science and Culture, Japan (No. 08554026).

References

1 S. F. Mason and D. R. Roberts, *J. Chem. Soc., Chem. Commun.*, 1967, 476.
2 R. A. Henry and C. A. Heller, *J. Luminescence*, 1971, **4**, 105.
3 C. A. Heller, R. A. Henry and J. M. Fritsch, in *Chemiluminescence and Bioluminescence*, ed. M. J. Cormier, D. M. Hercules and J. Lee, Plenum Press, New York, 1973, p. 249.
4 K. Maeda, Y. Matsuyama, K. Isozaki, S. Yamada and Y. Mori, *J. Chem. Soc., Perkin Trans. 2*, 1996, 121.
5 Y. Mori, Y. Matsuyama, S. Yamada and K. Maeda, *Acta Crystallogr., Sect. C*, 1992, **48**, 894.
6 Y. Mori, Y. Matsuyama, J. Suzuki, Y. Ishii, S. Yamada and K. Maeda, *Acta Crystallogr., Sect. C*, 1993, **49**, 1398.
7 K. Yamaguchi, Y. Ikeda and T. Fueno, *Tetrahedron*, 1985, **41**, 2099.
8 Z. Shi, V. Goulle and R. P. Thummel, *Tetrahedron Lett*., 1996, **37**, 2357.
9 D. T. Breslin and M. A. Fox, *J. Am. Chem. Soc*., 1993, **115**, 11716.
10 W. Adam and W. J. Baader, *J. Am. Chem. Soc*., 1985, **107**, 410.
11 G. B. Schuster, *Acc. Chem. Res*., 1979, **12**, 366.
12 L. H. Catalani and T. Wilson, *J. Am. Chem. Soc*., 1989, **111**, 2633.
13 For examples, W. Adam, R. Fell and M. H. Schulz, *Tetrahedron*, 1993, **49,** 2227; F. McCapra, *Tetrahedron Lett*., 1993, **34**, 6941.
14 R. S. Nicholson and I. Shain, *Anal. Chem*., 1964, **36**, 706.
15 M. Tsushima, K. Tokuda and T. Ohsaka, *Anal. Chem*., 1994, **66,** 4551.
16 G. Eberlein and T. C. Bruice, *J. Am. Chem. Soc*., 1983, **105**, 6685.
17 D. T. Sawyer and E. J. Nanni, in *Oxygen and oxy-radicals in chemistry and biology*, ed. M. A. Rodgers and E. L. Powers, Academic Press, New York, 1982, pp. 15–44.
18 E. J. Nanni, Jr., C. T. Angelis, J. Dickson and D. T. Sawyer, *J. Am. Chem. Soc*., 1981, **103**, 4268.
19 Y. Yoshioka, S. Yamanaka, S. Yamada, T. Kawakami, M. Nishino, K. Yamaguchi and A. Nishinaga, *Bull. Chem. Soc. Jpn*., 1996, **69**, 2701.
20 N. J. Turro, *Tetrahedron Lett*., 1985, **41**, 2089.
21 C. A. Heller, *Adv. Chem. Ser*., 1968, p. 225.
22 J. J. P. Stewart, *J. Comput. Chem*., 1989, **10**, 209.
23 J. E. Dickeson and L. A. Summers, *J. Heterocycl. Chem*., 1970, **7**, 401.
24 A. L. Rieger and P. H. Rieger, *J. Phys. Chem*., 1984, **88**, 5845.
25 C. S. Johnson, Jr., *Adv. Magn. Reson*., 1965, **1**, 33.
26 F. C. Adam, *Can. J. Chem*., 1971, **49**, 3524.
27 P. D. Sullivan and M. L. Williams, *J. Am. Chem. Soc*., 1976, **98**, 1711.
28 M. Tiecco, L. Testaferri, M. Tingoli, D. Chianelli and M. Montanucci, *Synthesis*, 1984, 736.
29 P. Desos, G. Schlewer and C. G. Wermuth, *Heterocycles*, 1989, **28**, 1085.
30 H. Balli and D. Schelz, *Helv. Chim. Acta*, 1970, **53**, 1903.
31 C. E. Kaslow and D. J. Cook, *J. Am. Chem. Soc*., 1945, **67**, 1969.
32 J. Lee and H. H. Seliger, *Photochem. Photobiol*., 1965, **4**, 1015.
33 J. J. P. Stewart, MOPAC Ver. 6.0, QCPE No. 455; Revised as Ver. 6.01 by T. Hirano, Ochanomizu University.

Paper 7/02289A
Received 3*rd April* 1997
Accepted 19*th June* 1997